Fractal Structure of Optical Anisotropy Mueller-Matrices Images of Biological Layers

A.V. Dubolazov[1], G.D. Koval[2], N.I. Zabolotna[3], S.V. Pavlov[3]

[1]Optics and Publishing Department, Chernivtsi National University,
2 Kotsyubinsky Str., Chernivtsi, 58012, Ukraine

[2]Bukovinian State Medical University, Chernivtsi, 58012, Ukraine

[3] Vinnitsa Technical National University, Vinnitsa, Ukraine
o.ushenko@chnu.edu.ua

ABSTRACT

The basic crystal optical mechanisms of formation of polarizable singularity images of polycrystalline networks of body fluid films with slight phase fluctuations were determined. Coordinate allocation of L-states is conditioned by the interaction of laser radiation with the substance of optically active proteins; C-states form on account of the phase modulation of orderly acicular protein crystals. On this basis the new Mueller-matrices method of diagnostics and differentiation of the changes of birefringence of body fluid films was developed and nosology differentiation was carried out for the first time. The results of the comparative study of the diagnostic effectiveness of the use of statistic, correlation, and fractal analysis of allocation of the characteristic meanings of the phase Mueller-matrices images in the differentiation of the polycrystalline film structure changes of body fluids were given.

Key words: polarimetry, Mueller matrix, laser, biological tissues.

1. Introduction

There is a wide range of biological objects for which the methods of laser and Mueller-matrices polarimetry haven't been widely used [1-3]. In the first place these are various body fluids (blood and its plasma, urine, bile, synovial fluid, perspiration of human organs etc.). From the medical point of view such objects are more accessible for in vitro laboratory examinations compared to histological biopsy sections of biological tissues. Moreover getting the experimental fluid samples (films dried at room temperature and applied to optically homogeneous glass) is much easier and doesn't require the traumatic biopsy operations. These circumstances ensure the possibility of a more simple and quick monitoring of the polycrystalline structure changes caused by the appearance of pathological changes, along with diagnostics of the disease as well as diagnostics of the treatment effectiveness.

The method of differentiation of polarizable qualities of human blood plasma smears with the following nosologies was suggested:

- healthy person (donor) – group 1;
- person with an inflammatory process (knee-joint inflammation) – group 2;
- person with cancer (uterus adenocarcinoma) – group 3.

2. The structure of the allocation of the characteristic meanings of the phase Mueller-matrices images of the albumin-globulin polycrystalline networks

For a more detailed study out of the whole coordinate set of meanings of Mueller-matrices images $m_{44}(x,y)$ of plasma smears of all the groups (fragments (a)) samples of characteristic meanings determining formation of the L-states $\left(m_{44}(x,y)=1\right)$ – (fragments (b)) and the C-states $\left(m_{44}(x,y)=0\right)$ – (fragments (c)) were found – fig. 1-3. [4].

Comparative analysis of the coordinate networks of the characteristic meanings [5-21] of the element of Mueller's matrix characterizing the phase anisotropy of the polycrystalline protein networks of human blood plasma films with

Eleventh International Conference on Correlation Optics, edited by Oleg V. Angelsky, Proc. of SPIE
Vol. 9066, 90661W · © 2013 SPIE · CCC code: 0277-786X/13/$18 · doi: 10.1117/12.2053848

various types of nosology showed their differences on the extreme levels $(m_{44}(x,y)=0)$ - (fragments (c)) - fig. 1-3.

Proceeding from this the allocation of the characteristic meanings $N^{(0)}(x)=(N^{(1)},N^{(2)},...,N^{(m)})$ of the Mueller-matrices images $m_{44}(x,y)$ was analyzed in detail using statistical, correlation, and fractal approaches.

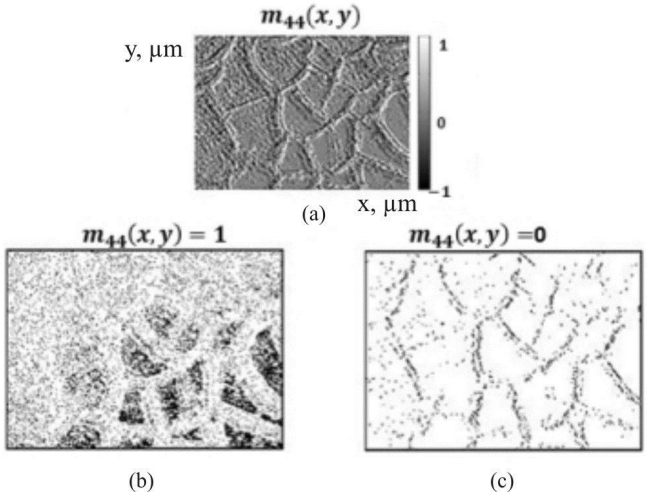

Figure. 1. Coordinate allocation of Mueller-matrices images $m_{44}(x,y)$ (a) and their characteristic meanings $(m_{44}(x,y)=1)$, (b) and $(m_{44}(x,y)=0)$, (c) of the first blood group plasma smear.

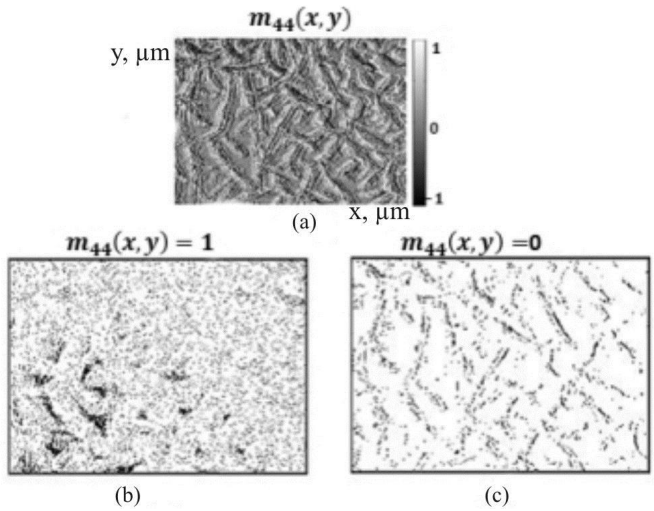

Figure. 2 Coordinate allocation of Mueller-matrices images $m_{44}(x,y)$ (a) and their characteristic meanings $(m_{44}(x,y)=1)$, (b) and $(m_{44}(x,y)=0)$, (c) of the of the second blood group plasma smear.

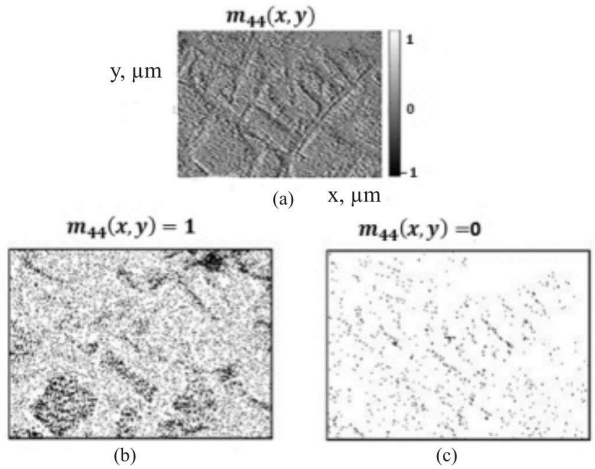

Figure. 3 Coordinate allocation of Mueller-matrices images $m_{44}(x,y)$ (a) and their characteristic meanings $(m_{44}(x,y)=1)$, (b) and $(m_{44}(x,y)=0)$, (c) of the third blood group plasma smear.

Figures. 4-6 show the results of the experimental study:

- frameworks coordinate distributions of the characteristic value of the Muller-matrix phase transformed image $(m_{44}(x,y)=1)$ fragments (a);
- the distribution of the number of the following value $N^{(1)}(x)=(N^{(1)},N^{(2)},...,N^{(m)})$ fragments (b);
- autocorrelation correspondences, that characterize the distributions $N^{(1)}(x)=(N^{(1)},N^{(2)},...,N^{(m)})$ fragments (c);
- the logarithmic dependence for the power disposal spectrum $N^{(1)}(x)=(N^{(1)},N^{(2)},...,N^{(m)})$ fragments (d);
- the analogical data for the sampling $(m_{44}(x,y)=0)$ and distribution $N^{(0)}(x)=(N^{(1)},N^{(2)},...,N^{(m)})$ as illustrated in fig. 5-9.

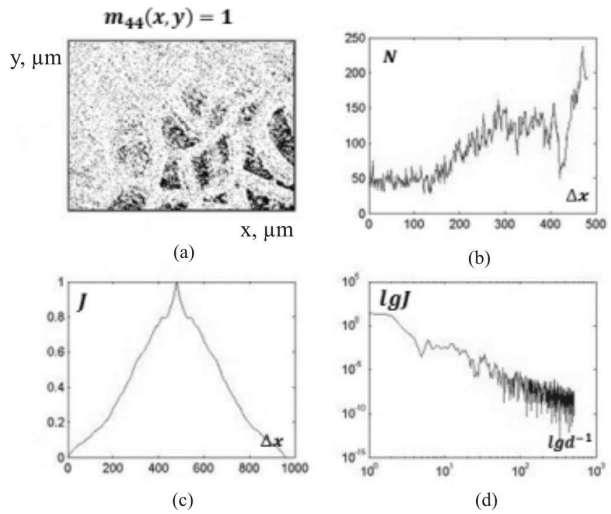

Figure. 4. Coordinate (a), quantitative (b), correlation (c) and special-frequency (d) parameters of the characteristic values $(m_{44}(x,y)=1)$ the Muller-matrix phase transformed image species of blood plasma of blood group O

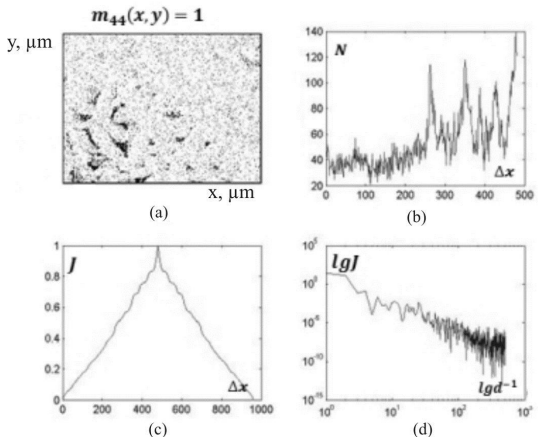

Figure. 5. Coordinate (a), quantitative (b), correlation (c) and special-frequency (d) parameters of the characteristic values $(m_{44}(x,y)=1)$ the Muller-matrix phase transformed image species of blood plasma of blood group A

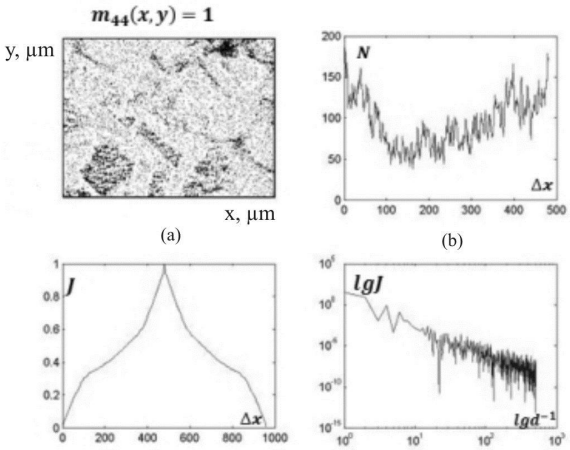

Figure. 6. Coordinate (a), quantitative (b), correlation (c) and special-frequency (d) parameters of the characteristic values $(m_{44}(x,y)=1)$ Muller-matrix phase transformed image species of blood plasma of blood group B

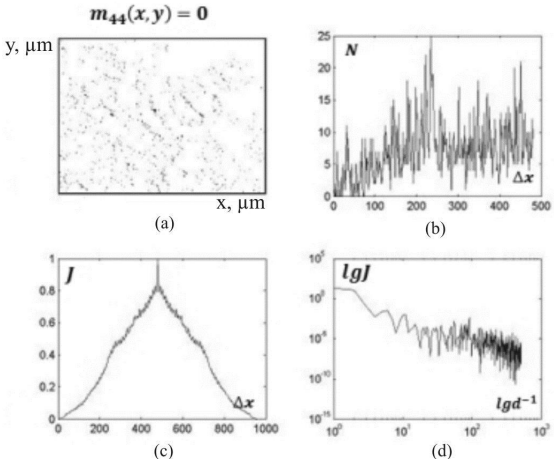

Figure. 7. Coordinate (a), quantitative (b), correlation (c) and special-frequency (d) parameters of the characteristic values $(m_{44}(x,y)=0)$ the Muller-matrix phase transformed image species of blood plasma of blood group C

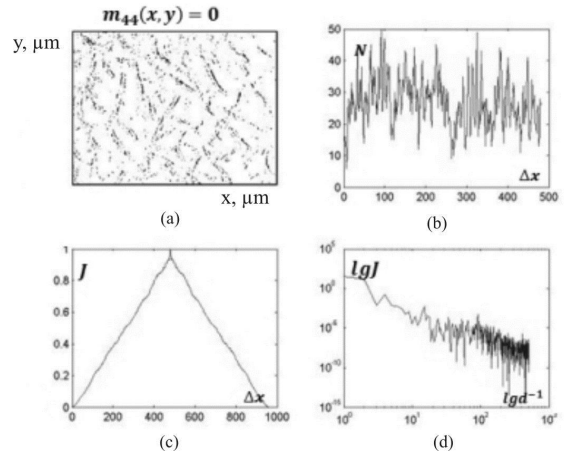

Figure. 8. Coordinate (a), quantitative (b), correlation (c) and special-frequency (d) parameters of the characteristic values $(m_{44}(x,y)=0)$ the Muller-matrix phase transformed image species of blood plasma of blood group A

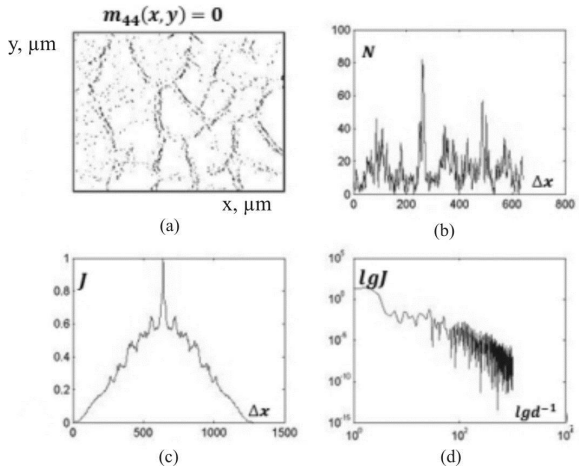

Figure. 9. Coordinate (a), quantitative (b), correlation (c) and special-frequency (d) parameters of the characteristic values $(m_{44}(x,y)=0)$ the Muller-matrix phase transformed image species of blood plasma of blood group B

The parameters comparative analysis of the topographic texture of characteristic value $(m_{44}(x,y)=1)$ the Muller-matrix phase transformed images $m_{44}(x,y)$ the polycrystalline texture of the proteins form the surface of blood plasma which occurred in different types of nosology:

- Within the statistical approach the distributions are quite similar $N^{(1)}(x)=(N^{(1)},N^{(2)},...,N^{(m)})$ samplings of the characteristic value $(m_{44}(x,y)=1)$ fig. 4-6, (fragments (a)) Muller-matrix phase item $m_{44}(x,y)$, that characterizes optically-isotropic texture of the blood plasma smears (fig. 4-6, fragments (b)). This fact testifies for practically similar and quite independent from the state of organism of the concentration content of all optically-isotropic biochemical substances.
- Within the correlation approach - autocorrelation distributional functions $N^{(1)}(x)=(N^{(1)},N^{(2)},...,N^{(m)})$ of the Muller-matrix characteristic value phase elements of the samples of blood plasma surface of all blood groups which used to be monotonous and smoothly falling off causation (fig. 4-6, fragment (c)). This fact points to the high level of coordinative equal optically –isotropic texture $N^{(1)}(x)=(N^{(1)},N^{(2)},...,N^{(m)})$ in the smears plane.
- Within the fractal approach - logarithmic dependence of the spectrum power disposal $N^{(1)}(x)=(N^{(1)},N^{(2)},...,N^{(m)})$ of the characteristic value of Muller-matrix phase transformed image of the blood plasma surface of all blood groups are permanent and similarly bent curves within three decades the changes of geometrical size (fig. 4-6,

fragments (d)). Having founded peculiarity points to the large scale similarity or fractal structure of the optically-isotropic texture of the blood plasma samples with different nosology.

Quantity parameters objectively characterizing divisions $N^{(1)}(x)=\left(N^{(1)},N^{(2)},...,N^{(m)}\right)$ given in a table 1.

Table 1. Statistical, correlative and fractional parameters of the sample $\left(m_{44}(x,y)=1\right)$ of the Muller-matrix images of blood plasma pellicles

$Z_{i=1,2,3,4}$	Healthy *(q=21)*	Inflammation *(q=20)*	Cancer *(q=19)*
Z_1	*0,54±0,11*	*0,58±0,12*	*0,51±0,13*
Z_2	*0,15±0,023*	*0,17±0,023*	*0,14±0,018*
Z_3	*0,68±0,091*	*0,77±0,11*	*0,72±0,13*
Z_4	*0,47±0,061*	*0,58±0,15*	*0,63±0,12*
K_2	*0,19±0,022*	*0,31±0,033*	*0,31±0,033*
K_4	*0,89±0,099*	*2,64±0,27*	*2,64±0,27*
D	*0,27±0,033*	*0,18±0,023*	*0,18±0,023*

From the data analysis, given in a table 1, one can notice that statistical, correlative and scale like topographic structure of phase Muller-matrix image of the optical-isotropic component of the samples of blood plasma pellicles of different nosology groups is practically identical.

Comparative analysis of the topographical structure parameters of the characteristic meanings $\left(m_{44}(x,y)=0\right)$ of the optical-anisotropic component of the Muller-matrix images $m_{44}(x,y)$ of the polycrystalline protein chains of blood plasma pellicles with different nosology types revealed diagnostic sensibility of the given method to the change of double refraction, caused by the rise of pathological states of a human organism:

- Within the scope of the statistical approach - the distributions $N^{(0)}(x)=\left(N^{(1)},N^{(2)},...,N^{(m)}\right)$ of representative values $\left(m_{44}(x,y)=0\right)$ (fig. 7 - 9, fragments (a)) of the phase matrix element sample which characterizes optically anisotropic linearly and circularly birefringent component of the blood plasma films (fig. 7-9, fragments (b)) are individual and essentially differ from each other. It is determined that for the inflammatory process the average number of characteristic values $\left(m_{44}(x,y)=0\right)$ in the plane of blood plasma film of a person with the inflammatory process increases 1,5 times (fig. 8, fragment (b)). For the oncological state (uterine wall adenocarcinoma) - it increases 2,2 times (fig. 9, fragment (b)). The discovered fact indicates the increase of the birefringence of albumin-globulin polycrystalline network of blood plasma proteins when appearing of the pathological states of a human organism.
- Within the correlation approach - autocorrelation distributional functions $N^{(0)}(x)=\left(N^{(1)},N^{(2)},...,N^{(m)}\right)$ of the charactenstic values $\left(m_{44}(x,y)=0\right)$ of the blood plasma samples of all blood groups are transformed and appears to be swiftly falling down causations with "sharp" peak (fig. 7 - 9, fragments (a)). Such peculiarity of the autocorrelation dependence points to the coordinate disorder of the phase shifting which are formed with the optically -anisotropic texture that are characterized with the divisions $N^{(0)}(x)=\left(N^{(1)},N^{(2)},...,N^{(m)}\right)$ in the smears plane of all blood groups.
- Within the fractal approach - logarithmic dependence of the power disposal spectrum divisions $N^{(0)}(x)=\left(N^{(1)},N^{(2)},...,N^{(m)}\right)$ of the characteristic values $\left(m_{44}(x,y)=0\right)$ of the samples of blood plasma plane of all blood groups are statistic without clearly shown banded angle of the approximating curve within three decades of the geometrical shape changes (fig. 7-9 fragment (d)). Having founded peculiarity points to the set up of the shifting phase which was formed with the optical-isotropic texture spaces of blood plasma with different nosology.

The quantitative values which objectively characterize distributions $N^{(0)}(x)=\left(N^{(1)},N^{(2)},...,N^{(m)}\right)$ the characteristic values of phase Muller-matrix image of the birefringence component in the dabs of plasma (from three patients groups) are given in table 2.

Table 2. Statistic, correlation, and fractal parameters of the sample $(m_{44}(x,y)=0)$ of phase Muller-matrix image of plasma films

$Z_{i=1,2,3,4}$	Healthy *(q=21)*	Inflammation *(q=20)*	Cancer *(q=19)*
Z_1	*0,22±0,028*	*0,36±0,042*	*0,43±0,054*
Z_2	*0,23±0,03*	*0,13±0,017*	*0,095±0,012*
Z_3	*0,89±0,091*	*2,17±0,27*	*3,67±0,48*
Z_4	*0,77±0,081*	*2,86±0,31*	*4,18±0,53*
K_2	*0,19±0,022*	*0,31±0,033*	*0,32±0,0337*
K_4	*0,89±0,099*	*2,64±0,27*	*4,16±0,57*
D	*0,27±0,033*	*0,18±0,023*	*0,4±0,019*

It is established that static moments of 3d and 4th order and the excess of autocorrelation are diagnostically sensitive. The difference between them is 2,4 and 4,1 times, 2,7 times.

With the aim to use the given method clinically the stated parameters of sensitivity Φ and specificity Ψ of the research in the limits of the chosen groups of blood pellicles are defined.

$$\Phi = \frac{a-b}{a+b}\cdot 100\% \tag{1}$$

$$\Psi = \frac{c-d}{c+d} \tag{2}$$

For the biomedical research the high levels of sensitivity (Φ=75%) and specificity (Ψ=70%) of the Muller-matrix mapping of the characteristic values of the phase component of the polycrystalline network of the protein pellicles of the blood plasma.

3. Conclusions:

1. The model of the polycrystalline structure of the blood plasma pellicles is presented in the aggregate of double refractive proteins of albumen and globulin is set.
2. The method of static, correlation and fractal characteristic values distribution analysis of the Muller-matrix images of the blood plasma double refractive pellicles is developed.
3. Established diagnostic effectiveness of determination of statistical moments of 1 - 4 order which characterize divisions of character meanings of phase Mueller-matrix image of blood plasma membranes in the differentiation of their polycrystalline human systems.
4. Applied for the first time complex statistical, correlation and fractal characteristic values distribution analysis of the Muller-matrix images of linearly and circularly two-beam-refracted albumen-globulin systems of blood plasma membranes with three types of nosology: norm - inflammation - cancer.

REFERENCES

[1] Ushenko, Yu., A., Angelsky, O.,V., Dubolazov, A., V., Telenha, O.,Yu., "The Interconnection between the Coordinate Distribution of Mueller-Matrixes Images Characteristic Values of Biological Liquid Crystals Net and the Pathological Changes of Human Tissues," Advances in Optical Technologies (ID 130659), P.1-10 (2010).

[2] Ushenko, Yu.,O., Misevich, I.,Z., Angelsky, A.P., Bachinsky, V.,T., Telen'ga, O.,Yu., Olar, O.,I., "Polarization-singular structure in laser images of phase-inhomogeneous layers to diagnose and classify their optical properties," Semicond. Physics, Quantum Electronics&Optoelectronics 13(3), P. 248-258 (2010).

[3] Ushenko, Yu.,O., Telenha, O., Balanetskyaya, V., "Laser metrology of biological liquid crystals singular structure," Proc. SPIE 7821, P. 78210Z (2010).

[4] Ushenko, Yu., O., Tomka, Yu.,Ya., Telenga, O., I., Misevitch, I., Z., Istratiy, V., V., "Complex degree of mutual anisotropy of biological liquid crystals nets," Opt. Eng. 50, P. 039001 (2011).

[5] Ushenko, Yu.,A., Tomka, Yu.,Ya., Dubolazov, A.,V., Telenga, O.,Yu., "Diagnostics of optical anisotropy

changes in biological tissues using Müller matrix," QUANTUM ELECTRON 41(3), P. 273–277 (2011).
[6] Ushenko, Yu., O., Telenga, O., Y., "Polarization-singular processing of biological layers laser images to diagnose and classify their optical properties," Proc. SPIE 8338, P. 83380U (2011).
[7] Ushenko, Yu., A., Misevich, I., Z., Telenga, O., Yu., Angelsky, A., P., "Potentiality of using the singular approach for analysis of rough surfaces polarization-inhomogeneous laser images in diagnostics and classification of their optical properties," Opt. Eng. 51, P. 014301 (2012).
[8] Dubolazov, A.,V., Telenha, O.,Y., Ushenko, V., A., Sydor, M., "Characteristic values of Mueller-matrixes images of biological liquid crystals net for diagnostics of human tissues anisotropy," Proc. SPIE 8338, P. 83380Z (2011).
[9] Koval, G.,D., Raranskiy, M.,D., "System of space-frequency filtering of linear and circular birefringence in cancer diagnosis." Proc. SPIE 8842 (Novel Optical Systems Design and Optimization XVI), 884212 (2013).
[10] Ushenko, Yu.,A., Dubolazov, A.,V., Angelsky, A., P., Sidor, M., I., Bodnar, G., B., Koval, G., Zabolotna, N., I., Smolarz, A., Junisbekov, M., Sh., "Laser polarization fluorescence of the networks of optically anisotropic biological crystals." Proc. SPIE (Optical Fibers and Their Applications), 869809 (2012).
[11] Angel'skii, O.,V., Ushenko, A.,G., Arkhelyuk, A.,D.,, Ermolenko, S.,B.,, Burkovets, D.,N., "Scattering of laser radiation by multifractal biological structures," Optika i Spektroskopiya 88 (3), 495-498 (2000).
[12] Angel`skii, O.,V., Ushenko, O.,G., Burkovets, D.,N., Arkhelyuk, O.,D., Ushenko, Y.,A., "Polarization-correlation studies of multifractal structures in biotissues and diagnostics of their pathologic changes." LASER PHYSICS 10(5), 1136-1142 (2000).
[13] Angelsky, O.,V., Maksimyak, P.,P., Hanson, S.,G., Ryukhin, V.,V., "New Feasibilities for Characterizing Rough Surfaces by Optical-Correlation Techniques," Applied Optics 40, pp. 5693-5707 (2001).
[14] Angelsky, O.,V., Hanson, S., G., Zenkova, C.,Yu., Gorsky, M.,P., Gorodyns'ka, N.,V., "On polarization metrology (estimation) of the degree of coherence of optical waves." Optics Express 17(18), pp.15623-15634 (2009).
[15] Angelsky, O.,V., Ushenko, A.,G., Burkovets, D.,N., Ushenko, Y.,A., "Polarization visualization and selection of biotissue image two-layer scattering medium," Journal of biomedical optics 10(1), P.14010 (2005).
[16] Angelsky, O.,V., Bekshaev, A.,Ya., Maksimyak, P.,P., Maksimyak, A.,P., Mokhun, I.,I., Hanson, S.,G., Zenkova, C., Yu., Tyurin, A.,V., "Circular motion of particles suspended in a Gaussian beam with circular polarization validates the spin part of the internal energy flow." Optics Express 20(10), pp.11351-11356 (2012).
[17] Brus, V., Pidkamin, L.,J., Abashin, S.,L., Kovalyuk, Z.,D., Maryanchuk, P.,D., Chugai, O.,M., "Optical constants and polarimetric properties of TiO2–MnO2 thin films." Optical Materials (34), 1940–1945 (2012).
[18] Ushenko, Y.,A., Dubolazov, O.,V., Karachevtsev, A.,O., "Statistical structure of skin derma Mueller matrix images in the process of cancer changes." Optical Memory & Neural Networks 20 (2), p.145-154 (2011).
[19] Angelsky, O.,V., Burkovets, D.,N., Maksimyak, P.,P., Hanson, S.G., "Applicability of the singular-optics concept for diagnostics of random and fractal rough surfaces," Applied optics 42 (22), 4529-4540 (2003).
[20] Angelsky, O.,V., Yermolenko, S.,B., Zenkova, C.,Yu., Angelskaya, A.,O., "Polarization manifestations of correlation (intrinsic coherence) of optical fields." Applied optics 47 (29), 5492-5499 (2008)
[21] Angelsky, O., Mokhun, A., Mokhun, I., Soskin, M., "The relationship between topological characteristics of component vortices and polarization singularities," Optics communications 207 (1), 57-65 (2002).